

AD-755 808

DIURNAL CYCLES OF THE REFRACTIVE INDEX
STRUCTURE FUNCTION COEFFICIENT

Marvin L. Wesley, et al

Ballistic Research Laboratories

Prepared for:

Army Materiel Command

November 1972

DISTRIBUTED BY:

NTIS

National Technical Information Service
U. S. DEPARTMENT OF COMMERCE
5285 Port Royal Road, Springfield Va. 22151

BRL MR 2243

BRL

AD

AD 755808

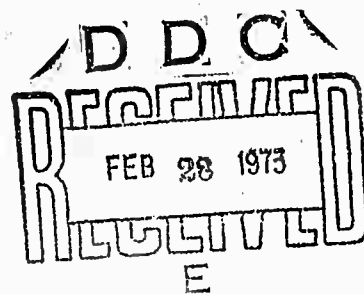
MEMORANDUM REPORT NO. 2243

DIURNAL CYCLES OF THE REFRACTIVE INDEX STRUCTURE FUNCTION COEFFICIENT

by

Marvin L. Wesely
Ernest C. Alcaraz

November 1972



Approved for public release; distribution unlimited.

Reproduced by
NATIONAL TECHNICAL
INFORMATION SERVICE
U S Department of Commerce
Springfield VA 22151

USA BALLISTIC RESEARCH LABORATORIES
ABERDEEN PROVING GROUND, MARYLAND

R
33

Destroy this report when it is no longer needed.
Do not return it to the originator.

Secondary distribution of this report by originating or
sponsoring activity is prohibited.

Additional copies of this report may be purchased from
the U.S. Department of Commerce, National Technical
Information Service, Springfield, Virginia 22151

ACCESSION for	
NTIS	White Section <input checked="" type="checkbox"/>
DDC	Buff Section <input type="checkbox"/>
UNANNOUNCED	<input type="checkbox"/>
JUSTIFICATION	
BY	
DISTRIBUTION/AVAILABILITY CODES	
DISC.	EXCL. COPY & SPECIAL
<i>A</i>	

The findings in this report are not to be construed as
an official Department of the Army position, unless
so designated by other authorized documents.

Unclassified

Security Classification

DOCUMENT CONTROL DATA - R & D

(Security classification of title, body of abstract and indexing annotation must be entered when the overall report is classified)

1. ORIGINATING ACTIVITY (Corporate author) U.S. Army Ballistic Research Laboratories Aberdeen Proving Ground, MD 21005		2a. REPORT SECURITY CLASSIFICATION Unclassified	
		2b. GROUP	
3. REPORT TITLE DIURNAL CYCLES OF THE REFRACTIVE INDEX STRUCTURE FUNCTION COEFFICIENT			
4. DESCRIPTIVE NOTES (Type of report and inclusive dates)			
5. AUTHOR(S) (First name, middle initial, last name) Marvin L. Wesely, CPT USAR, and Ernest C. Alcaraz			
6. REPORT DATE November 1972		7a. TOTAL NO. OF PAGES 39	7b. NO. OF REFS 35
8a. CONTRACT OR GRANT NO. b. PROJECT NO. RDT&E IT563611D459 IT061102B11A c. d.		9a. ORIGINATOR'S REPORT NUMBER(S) BRL Memorandum Report No.2243 9b. OTHER REPORT NO(S) (Any other numbers that may be assigned this report)	
10. DISTRIBUTION STATEMENT Approved for public release; distribution unlimited.			
11. SUPPLEMENTARY NOTES This material was presented at a meeting of the IRIS Specialty Gp on IR Backgrounds & Atmospheric Physics at the NBS, Gaithersburg, MD, 18 May 72.		12. SPONSORING MILITARY ACTIVITY U.S. Army Materiel Command Washington, DC	
13. ABSTRACT The refractive index structure function coefficient, C_n^2 , is an atmospheric parameter needed to describe scintillation and small-scale phase ⁿ fluctuations of electromagnetic radiation propagated in the atmospheric surface layer. Since systematic direct measurements of C_n for many climates and seasons are not available, an indirect method is developed where C_n is calculated from the estimates of sensible and latent heat flux components of the surface energy budgets. This indirect method is primarily for heights less than 4 meters, because low intermittency and $K_H/K_M \approx 1$ are assumed. Diurnal variations of C_n at several heights above land for six combinations of climates, seasons, and surface conditions are calculated from heat fluxes measured by different investigators at many locations, for moderate to high wind velocities. These predictions of C_n agree well with some direct measurements of C_n when assumptions of nearly ideal weather and sites are met. The effect of water vapor on C_n is usually a reduction of about 3/8 per cent and thus is usually negligible above land, but can be significant above tropical oceans.			

DD FORM 1473
1 NOV 66

REPLACES DD FORM 1473, 1 JAN 64, WHICH IS
OBSOLETE FOR ARMY USE.

1a

Unclassified

Security Classification

Unclassified
Security Classification.

14. KEY WORDS	LINK A		LINK B		LINK C	
	ROLE	WT	ROLE	WT	ROLE	WT
Scintillation Imaging Refractive Index Structure Function Micrometeorology Turbulence						

16
Unclassified

Security Classification

BALLISTIC RESEARCH LABORATORIES

MEMORANDUM REPORT NO. 2243

NOVEMBER 1972

DIURNAL CYCLES OF THE REFRACTIVE INDEX STRUCTURE
FUNCTION COEFFICIENT

Marvin L. Wesely
Ernest C. Alcaraz

Concepts Analysis Laboratory

Approved for public release; distribution unlimited.

RDT&E Project No. IT563611D459
IT061102B11A

ABERDEEN PROVING GROUND, MARYLAND

2

BALLISTIC RESEARCH LABORATORIES

MEMORANDUM REPORT NO. 2243

MLWesely/ECAIcaraz/jdk
Aberdeen Proving Ground, Md.
November 1972

DIURNAL CYCLES OF THE REFRACTIVE INDEX STRUCTURE FUNCTION COEFFICIENT

ABSTRACT

The refractive index structure function coefficient, C_n^2 , is an atmospheric parameter needed to describe scintillation and small-scale phase fluctuations of electromagnetic radiation propagated in the atmospheric surface layer. Since systematic direct measurements of C_n for many climates and seasons are not available, an indirect method is developed where C_n is calculated from the estimates of sensible and latent heat flux components of the surface energy budgets. This indirect method is primarily for heights less than 4 meters, because low intermittency and $K_H/K_M \approx 1$ are assumed. Diurnal variations of C_n at several heights above land for six combinations of climates, seasons, and surface conditions are calculated from heat fluxes measured by different investigators at many locations, for moderate to high wind velocities. These predictions of C_n agree well with some direct measurements of C_n when assumptions of nearly ideal weather and sites are met. The effect of water vapor on C_n is usually a reduction of about 3/8 per cent and thus is usually negligible above land, but can be significant above tropical oceans.

TABLE OF CONTENTS

	Page
ABSTRACT.	3
LIST OF ILLUSTRATIONS	7
INTRODUCTION.	9
INDIRECT CALCULATION OF C_n	10
DIURNAL CYCLES OF C_n	17
CONCLUSION.	29
REFERENCES.	31
DISTRIBUTION LIST	35

LIST OF ILLUSTRATIONS

Figure		Page
1.	Dependence of C_T on z/L . The solid line was computed from equation 9	15
2.	C_T nondimensionalized with the local mean temperature gradient plotted against R_g . The solid line was computed from equation 10	15
3.	C_n vs mean solar time at 0.5, 2, 8, and 16 meters (top to bottom) for case 1	19
4.	C_n vs mean solar time at 0.5, 2, 8, and 16 meters (top to bottom) for case 2	20
5.	C_n vs mean solar time at 0.5, 2, 8, and 16 meters (top to bottom) for case 3	21
6.	C_n vs mean solar time at 0.5, 2, 8, and 16 meters (top to bottom) for case 4	22
7.	C_n vs mean solar time at 0.5, 2, 8, and 16 meters (top to bottom) for case 5	23
8.	C_n vs mean solar time at 0.5, 2, 8, and 16 meters (top to bottom) for case 6	24
9.	Test of case 2 with measurements made at the U. S. Army Ballistic Research Laboratories, January 29 and 30, 1972	25
10.	Test of case 3 with measurements made at the U. S. Army Ballistic Research Laboratories, May 27 and 28, 1971	26

INTRODUCTION

For optical radiation the atmospheric index of refraction variations primarily result from temperature-induced density changes. These variations cause scintillation and phase fluctuations of laser beams propagated in the atmosphere and the loss of resolution of objects viewed through high-magnification telescopes. Temperature variations also help cause the scattering of acoustic and radar signals, phenomena used in the remote sensing of the atmosphere. The length scales of the temperature inhomogeneities that distort image and laser beam propagation in the atmospheric surface layer are usually on the order of centimeters for scintillation and tens of centimeters for phase fluctuations, and the eddies with these sizes are in the inertial subrange where fluctuations are isotropic. Isotropy greatly aids the development of theories like those in *Tatarski* [1961] that describe electromagnetic propagation, and only one atmospheric parameter, the refractive index structure function coefficient, C_n^2 , is needed. Using Kolmogorov's theory one can determine C_n for optical radiation from a variance of temperature differences between two fast-response thermometers or from a temperature power spectrum at one thermometer. When the ideal case of the temperature and wind structure being horizontally homogeneous in the surface layer exists, one measurement suffices and C_n can be inferred for any height within a few meters of the surface.

The purpose of this paper is to present diurnal variations of C_n for optical radiation at several heights in the atmospheric surface layer for various climates, seasons, and surface characteristics. However, since direct systematic measurements of C_n are not available, an indirect method is developed, compared with similar indirect methods, and used to obtain diurnal trends. The indirect method uses sensible and latent heat flux components of the surface energy budgets, which have become abundantly available in the meteorological and climatological literature. Representative wind velocities are chosen and the effect of water vapor is evaluated. Also, the model developed

here is for use primarily at heights less than 4 meters, since the effect of intermittency at greater height limits the validity of necessary empirical functions.

Some of the terminology used in this paper must be explained. First, "turbulence" is not synonymous with "temperature fluctuations" as is common in atmospheric optics [Lawrence *et al.*, 1970]. It will be shown that water vapor fluctuations can be important relative to temperature fluctuations above a lake or an ocean. Also, wind velocity fluctuations can significantly affect the propagation of high-power laser beams. Thus "turbulence" implies any fluctuating property of the air, and equating a value of C_n with intensity of turbulence is misleading unless thermal turbulence is specified. Second, "stable" conditions refer to an inversion or an increase of potential temperature with height, and heat being convected from the air to the cooled ground. "Neutral" conditions are adiabatic conditions; C_n approaches zero and the average heat flux is zero. "Unstable" conditions are lapse conditions, or a decrease beyond the normal adiabatic decrease of temperature with height, and heat is being convected from the surface to the air.

INDIRECT CALCULATION OF C_n

The structure function, D_T , for temperature fluctuations is given by

$$D_T = \langle (T_1 - T_2)^2 \rangle, \quad (1)$$

where T_1 and T_2 are the temperatures at two points fixed on a line oriented normally to the mean wind direction and separated by distance r . Two thermometers can be used to measure T_1 and T_2 , but an alternative method is to use one thermometer and determine T_2 by lagging in time from T_1 by Δt . Then Taylor's Hypothesis of a frozen field is assumed and $r = \Delta t \bar{u}$, where \bar{u} is the mean longitudinal wind speed [Lumley and Panofsky, 1964]. When r is of the order of inertial

subrange scales, Kolmogorov's reasoning can be applied [Obukhov, 1949; Corrsin, 1951] to yield the following:

$$D_T = C_T^2 r^{2/3}, \quad (2)$$

where the coefficient is

$$C_T^2 = A N \epsilon^{-1/3}. \quad (3)$$

The value of A is constant, N is the rate of dissipation of temperature fluctuations, and ϵ is the rate of dissipation of mechanical turbulent energy.

Tatarski [1961] suggests that in a homogeneous, statistically stationary, atmospheric surface layer the rate of dissipation of temperature fluctuations is equal to the product of the vertical heat flux, H, and the mean vertical temperature gradient, $\partial \bar{T} / \partial z$. Data given by Wyngaard et al. [1971] indicate that this is a good assumption.

$$N = H \frac{\partial \bar{T}}{\partial z} (\rho C_p) \quad (4)$$

where (ρC_p) is the heat capacity of air and $H(\rho C_p) = \langle w'T' \rangle$ is the covariance of the vertical wind and temperature (the primes indicate deviations from the means). In the atmospheric surface layer, ϵ is the sum of mechanical and buoyant production rates of mechanical and turbulent energy [Lumley and Panofsky, 1964].

$$\epsilon = u_*^2 \frac{\partial \bar{u}}{\partial z} (1 - Rf) \quad (5)$$

where $u_* = \langle u'w' \rangle^{1/2}$ is the surface friction velocity, \bar{u} is the mean longitudinal wind speed, and Rf is the flux Richardson number. In this paper, terms that may cause equation 5 to be in error by up to 40 percent for non-neutral conditions [Record and Cramer, 1966; Zubkovskiy and Koprov, 1970; Wyngaard and Coté, 1970; McBean et al., 1971] are neglected because of disagreement about the sign and magnitude of the error terms. The value of A in equation 3 is obtained from temperature spectrum analyses and a representative value of 2.8 is used here [Panofsky, 1969; Pond et al., 1971; Wyngaard and Coté, 1971]. This value is very close

to the constant for the transverse wind structure function coefficient, but no theory states these constants must be the same. Since temperature is a scalar, there is no longitudinal form of equation 2 as exists for wind components, where the longitudinal constant is 3/4 the transverse constant.

Substituting equations 4 and 5 into equation 3, we find

$$C_T^2 = 2.8 \langle w'T' \rangle \frac{\partial \bar{T}}{\partial z} \left[u_*^2 \frac{\partial \bar{u}}{\partial z} (1-Rf) \right]^{-1/3} . \quad (6)$$

Lumley and Panofsky [1964] list several well-known relationships we can use to simplify equation 6.

$$\langle u'w' \rangle = K_M \frac{\partial \bar{u}}{\partial z} , \quad (7a)$$

$$\langle w'T' \rangle = K_H \frac{\partial \bar{T}}{\partial z} , \quad (7b)$$

where K_M and K_H are the eddy diffusivities for momentum and heat, respectively. The average wind speed and temperature gradients are

$$\frac{\partial \bar{u}}{\partial z} = \frac{u_*^* \phi_M}{kz} , \quad (8a)$$

$$\frac{\partial \bar{T}}{\partial z} = \frac{T^* \phi_H}{kz} , \quad (8b)$$

where $k = 0.4$ is von Karmon's constant, $T^* = \langle w'T' \rangle / u_*$, and ϕ_M and ϕ_H are the nondimensional shears of wind and temperature, respectively. Substitutions of equations 7 and 8 into equation 6 result in these final equations:

$$C_T z^{1/3} / T^* = 1.67 \phi_M^{1/2} \left[\alpha^{1/2} k^{1/3} (1-Rf)^{1/6} \right]^{-1} \quad (9)$$

and

$$C_T / \left(\frac{\partial \bar{T}}{\partial z} \right)^{2/3} = 1.67 k^{2/3} \alpha^{1/2} \left[\phi_M^{2/3} (1-Rf)^{1/6} \right]^{-1} , \quad (10)$$

where

$$\alpha = K_H/K_M = \phi_M/\phi_H .$$

Atmospheric variables can be nondimensionalized with u^* and T^* since they do not vary with height in the atmospheric surface layer. All properly nondimensionalized parameters can be characterized in terms of z/L where L is the Monin-Obukhov length.

$$z/L = zkgT^*(\bar{T}u^{*2})^{-1}, \quad (11)$$

where g is the acceleration of gravity. The right-hand sides of equations 9 and 10 have three parameters that must be evaluated as a function of z/L . The flux Richardson number is an explicit function of z/L : $Rf = \phi_M^{-1}z/L$. The function ϕ_M has been established by the empirical KEYPS function, but for computation purposes we choose to use the following:

$$\phi_M = 1+4.5(z/L) \quad (z/L > 0), \quad (12a)$$

$$\phi_M = 1+4.5(z/L)\exp(4.5z/L) \quad (0. > z/L \geq -0.04), \quad (12b)$$

$$\phi_M = 0.08+0.285(-z/L)^{1/3} \quad (z/L < -0.04). \quad (12c)$$

These equations result in curves of ϕ_M verses z/L that closely agree with those given by *Businger et al.* [1971]. For α , however, widely different estimates have been obtained [*Laykhtman and Ponomarev*, 1969; *Businger et al.*, 1971]. Here we will base our estimates on measurements described by *Wesely et al.* [1970] which were within 4 meters of the surface. The value of α was apparently near unity for all stability conditions since flux estimates from aerodynamic methods using $\alpha = 1$ agreed with direct flux estimates via eddy correlation techniques. The following forms for α are assumed:

$$\alpha = (1+2.25z/L) \quad (z/L > 0), \quad (13a)$$

$$\alpha = 1-0.225z/L \quad (z/L \leq 0). \quad (13b)$$

At heights greater than 4 meters, equation 13 is inaccurate since, as shown by *Haugen and Kaimal* [1971], intermittency increases with height and calculations by *Stearns* [1971] show that with highly intermittent conditions α becomes much larger than unity.

After substitution of equations 12 and 13 into equation 9, the curves in Fig. 1 can be calculated. Also shown is a curve determined from data collected at $z \geq 5.66$ meters, as summarized by *Wyngaard et al.* [1971]. The two curves differ because of the higher level of intermittency that existed at the greater height, thus increasing α or, alternatively, increasing T^* with respect to C_T in equation 9.

The value of C_T can also be determined from the mean gradients of temperature and horizontal wind rather than the fluxes of heat and momentum. This method uses the gradient Richardson number, R_g , as the stability parameter: $R_g = \phi_M^{-1} \alpha^{-1} z/L$. Substituting equations 12 and 13 into equation 10 results in Fig. 2, which also shows results from the same experiment cited for Fig. 1 ($z/L \geq 5.66$ meters). The effect of the increased level of intermittency at $z > 4$ meters is to increase the ordinate values because α is increased or, alternatively, $\frac{\partial T}{\partial z}$ is decreased with respect to C_T in equation 10. The remaining curve in Fig. 2 was determined by *Tsvang* [1960] from spectral analysis of temperature fluctuation measured at heights of 1 and 4 meters. Tsvang's curve appears low for unstable conditions ($R_g < 0$), as is also indicated by his comparisons with previous Russian estimates obtained with equation 1. Experimental data by *Livingston et al.* [1970] have shown that Tsvang's curve is reasonably accurate.

If only temperature changes significantly affect the air density and thus its refractive index,

$$C_n^2 = \left[A_1 p / \bar{T}^2 \right]^2 C_T^2, \quad (14)$$

where p is the static atmospheric pressure and A_1 is a constant for a particular radiation wavelength. However, fluctuations in water vapor

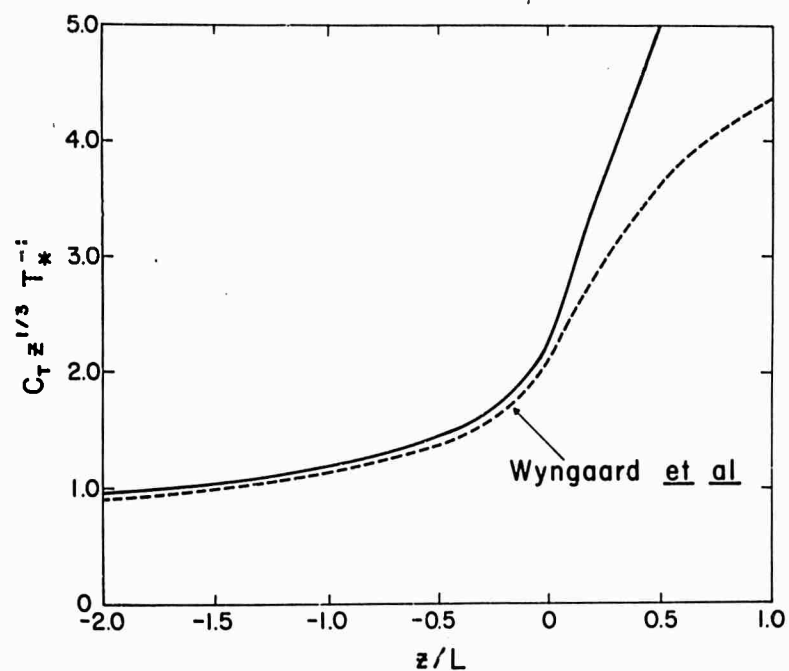


Figure 1 - Dependence of C_T on z/L . The solid line was computed from equation 9.

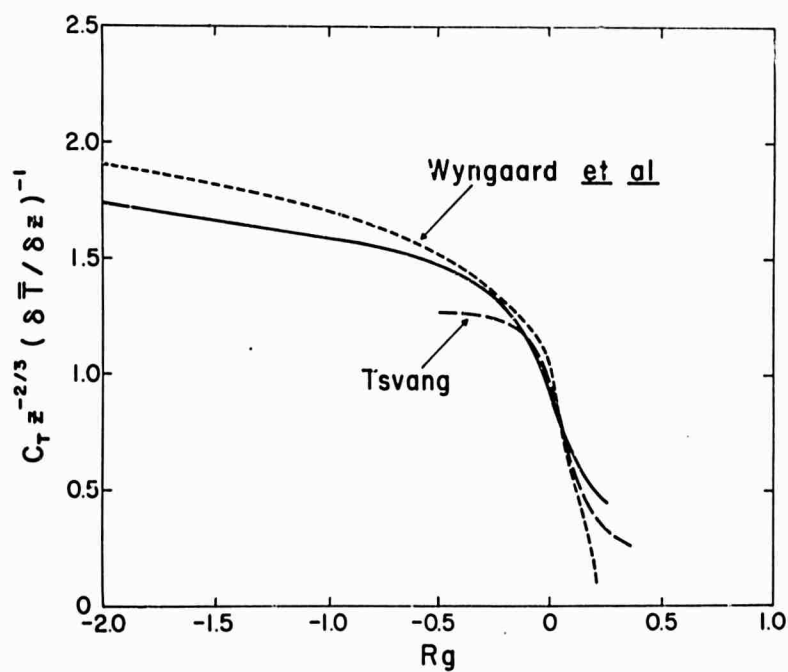


Figure 2 - C_T nondimensionalized with the local mean temperature gradient plotted against Rg . The solid line was computed from equation 10.

concentration can also affect air density. To evaluate this effect, we assume that the eddy diffusivities for scalar quantities are identical at any given time and location. This is justified by the success [e.g., *Wesely et al.*, 1970] of equating K_H with K_W , the eddy diffusivity for water vapor, in the Bowen's ratio method of computing vertical sensible and latent heat flux in the atmospheric surface layer [*Lumley and Panofsky*, 1964]. With replacement of T by n in equations 7b and 6 and the assumption of $K_n = K_H$, it can be shown that

$$C_n = C_T \langle w'n' \rangle / \langle w'T' \rangle \quad (15)$$

The atmospheric refractive index is given by *Fleagle* [1950] as

$$n - 1 = A_1 p / T + A_2 e / T,$$

where e is the water vapor pressure and A_2 is a constant for a particular radiation wavelength. Both A_1 and A_2 can be evaluated with the Barrell and Sears formula [*List*, 1958] using the technique described by *Kallistratova and Timanovsky* [1971]; $A_1 = 78.7 \times 10^{-6} \text{ }^\circ\text{K mb}^{-1}$ and $A_2 = 12.4 \times 10^{-6} \text{ }^\circ\text{K mb}^{-1}$ for a wavelength of 0.6μ . The value of A_1 varies only a few percent over the visible and near infrared spectrum, but A_2 varies greatly for different infrared wavelengths because of anomalous dispersion [*Chalfee*, 1968].

When pressure fluctuations and third order correlations are neglected, it can be shown that for visible light

$$\langle w'n' \rangle = -A_1 p \bar{T}^{-2} \langle w'T' \rangle [1 - \bar{T} A_2 C_p (0.622 A_1 V_B)^{-1}]. \quad (16)$$

Therefore, at $\bar{T} = 288^\circ\text{K}$ and $p = 1013 \text{ mb}$,

$$C_n = C_T A_1 p \bar{T}^{-2} [1 - 0.0298 \bar{T}^{-1}], \quad (17)$$

where V is the latent heat of vaporization and β is Bowen's ratio. Since $\beta = H/E$ where E is the latent heat flux, a high value of β in the daytime usually means that energy used in evaporation is much smaller than the thermal convective loss from the heated surface. This is the most frequent case above land since $\beta > 0.2$ is typical, and the correction in equation 17 is negligible there. Usually $\beta > 0$ because the earth's surfaces are most often either warming and evaporating or cooling and condensing; air parcels warmer than the surrounding air usually have a higher specific humidity. However, when surface cooling and evaporation occur simultaneously, $\beta < 0$ can be found above oceans and lakes when severe advection occurs and occasionally in a dry atmosphere above moist ground at night.

DIURNAL CYCLES OF C_n

Diurnal trends of C_n are shown in Figs. 3 through 8 for different micrometeorological conditions above land at middle latitudes. Hundreds of typical trends can occur, but a particular micrometeorological situation on a clear and cloudless day should yield either one of the diurnal trends shown here or something between two of the graphs. The variables that determine which curve to use are listed in Table 1, and they can be summarized as follows: (1) season and latitude, which determine the diurnal solar radiation cycle; (2) the amount of water available for evapotranspiration from the surface, whose main effect is to reduce the surface temperature rise; and (3) the radiation absorption characteristics of the surface, usually determined by the type and condition of vegetation, which is strongly dependent upon the above two factors and man's modifications. Another factor that must be taken into account is that C_n is approximately proportional to $1/u^*$. In Figs. 3 through 8, moderate wind speeds of about 3 m/sec at a 2-meter height ($u^* = 25 \text{ m/sec}$) are assumed when $H < 125 \text{ W m}^{-2}$, and strong wind speeds of about 5 m/sec at a 2-meter height ($u^* = 40 \text{ m/sec}$) are assumed when $H \geq 125 \text{ W m}^{-2}$.

TABLE 1. Assumed climatic conditions for C_n estimates in Figs. 3-8.

Case	Possible Climates			Season	Soil Moisture		
	Rainfall ^a	Latitude	Example		Subsurface	Surface	Surface
1	>25	30°-50°	Treeless area	Winter	Wet ^b	Wet ^b	Snow
2	>25	30°-50°	Treeless area	Winter	Wet ^b	Wet ^b	Short brown grass
3	75-125	30°-50°	Wet grasslands	Summer	Wet	Wet	Short green grass
4	50-100	30°-50°	Plains, steppes	Summer	Wet	Dry	Short green grass
5	<25	10°-40°	Desert	Winter	Dry	Dry	Bare sand, sparse or no plants
6	<25	10°-40°	Desert	Summer	Dry	Dry	

^acm/year

^bfrozen

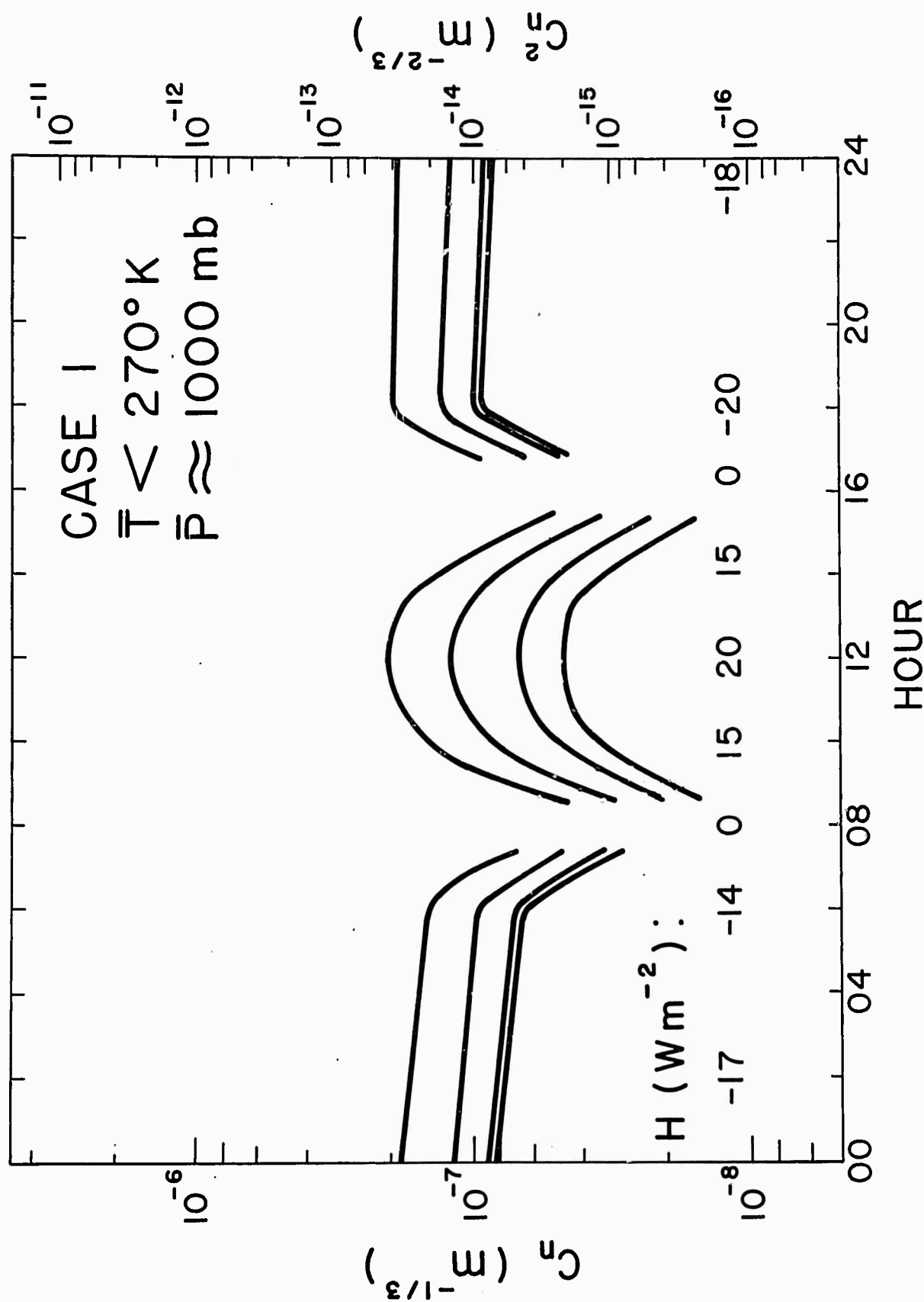


Figure 3 - C_n vs mean solar time at 0.5, 2, 8, and 16 meters (top to bottom) for case 1.

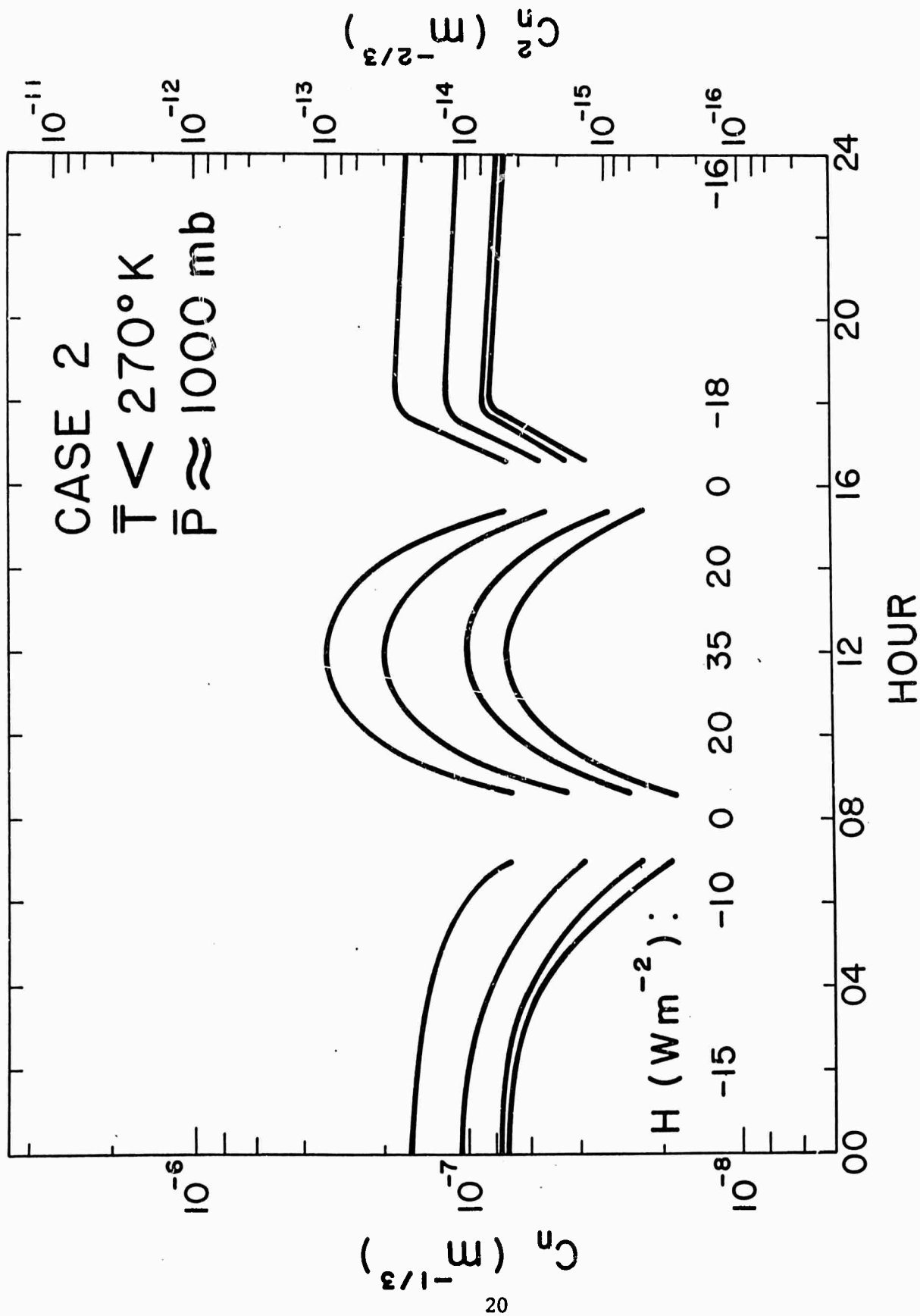


Figure 4 - C_n vs mean solar time at 0.5, 2, 8, and 16 meters (top to bottom) for case 2.

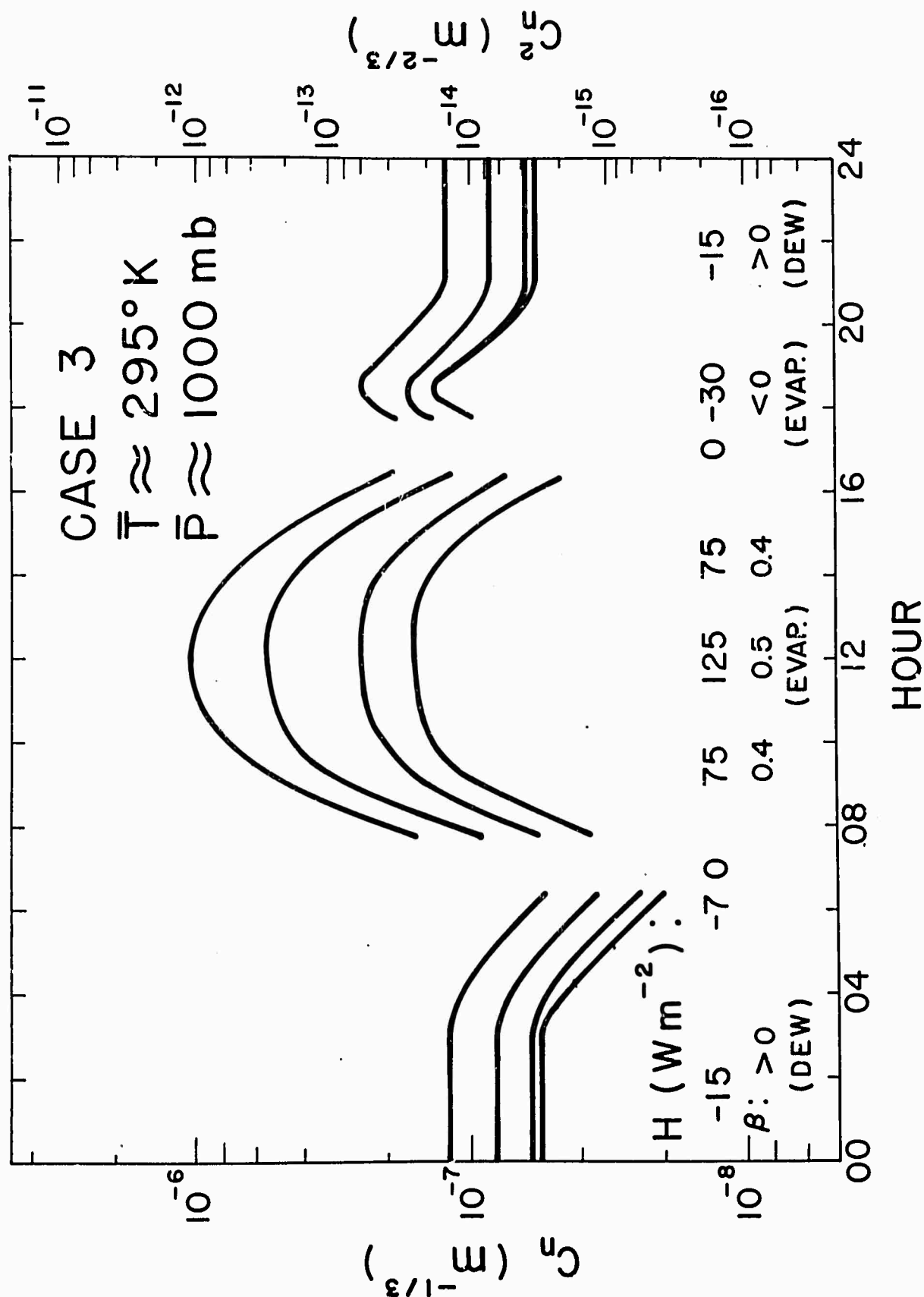


Figure 5 - C_n vs mean solar time at 0.5, 2, 8, and 16 meters (top to bottom) for case 3.

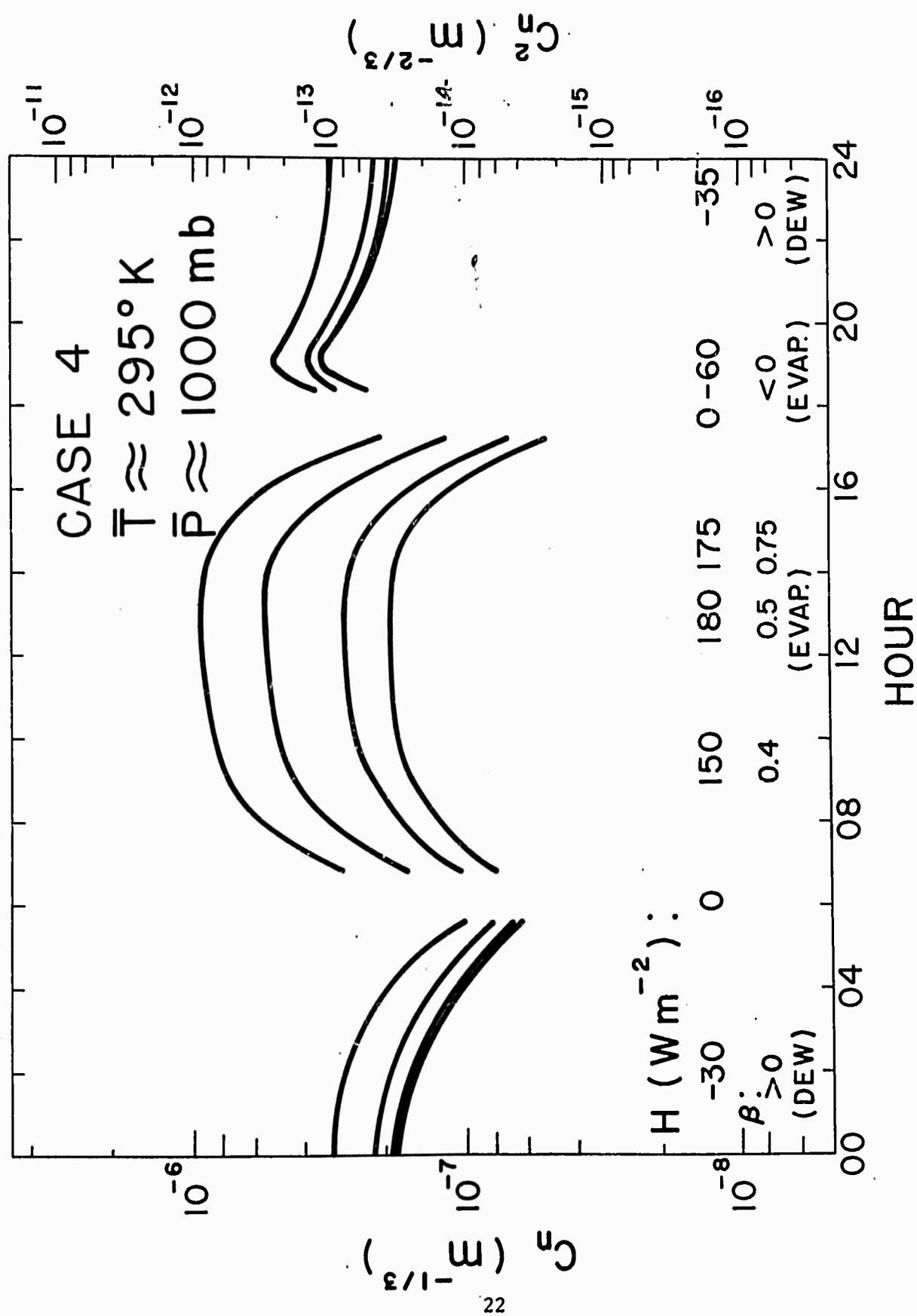


Figure 6 - C_n vs mean solar time at 0.5, 2, 8, and 16 meters (top to bottom) for case 4.

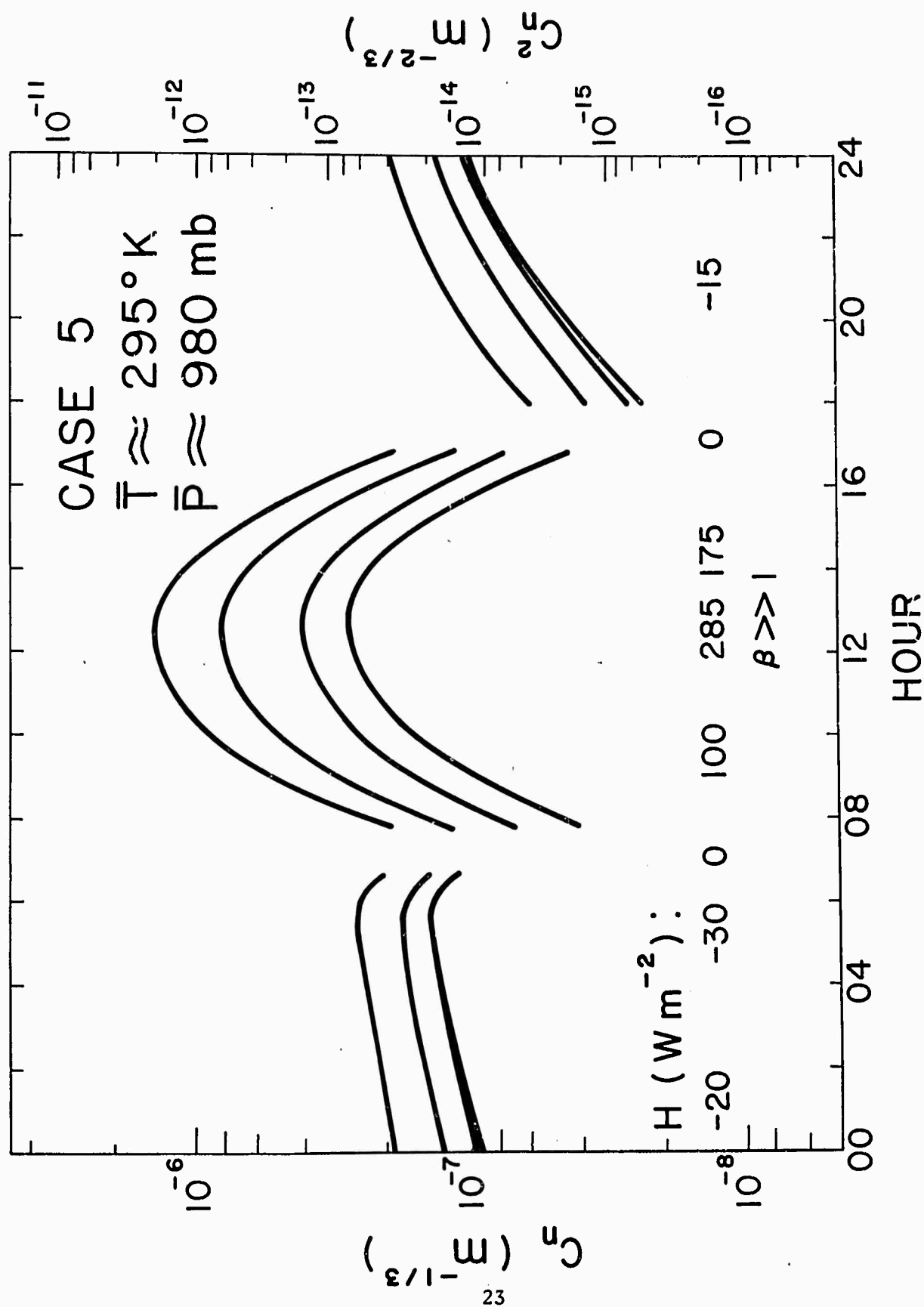


Figure 7 - C_n vs mean solar time at 0.5, 2, 8, and 16 meters (top to bottom) for case 5.

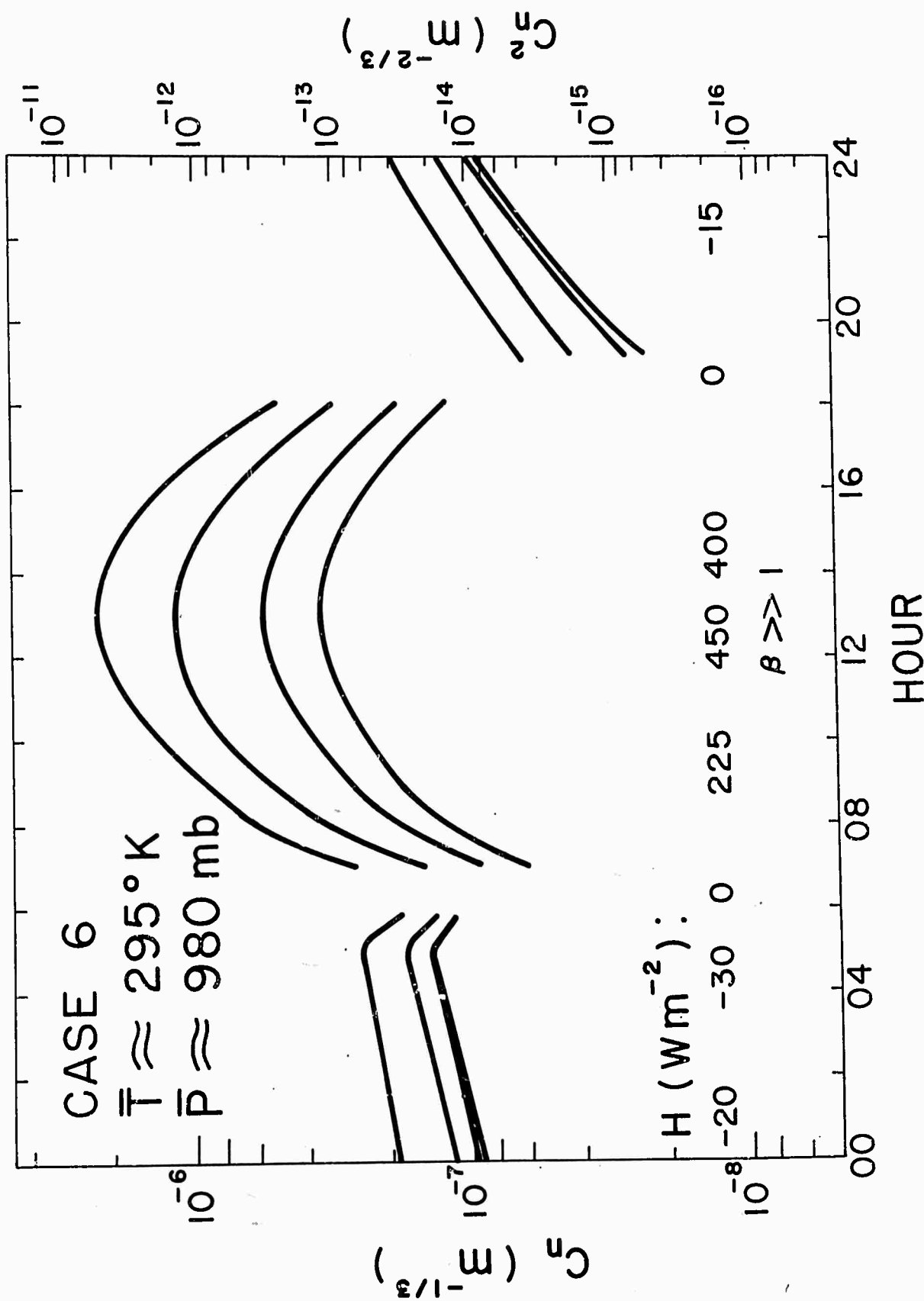


Figure 8 - C_n vs mean solar time at 0.5, 2, 8, and 16 meters (top to bottom) for case 6.

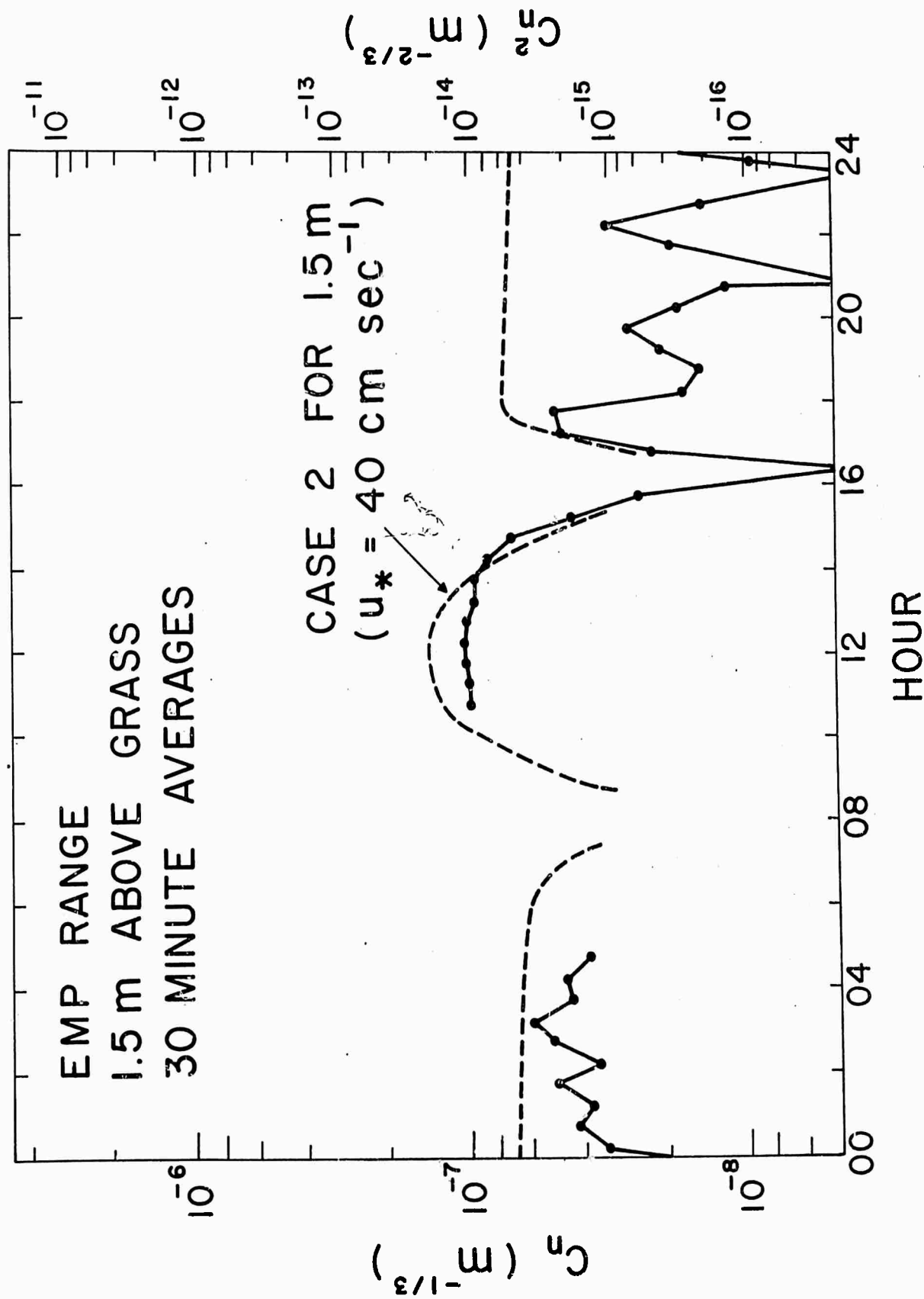


Figure 9 - Test of case 2 with measurements made at the U. S. Army Ballistic Research Laboratories, January 29 and 30, 1972.

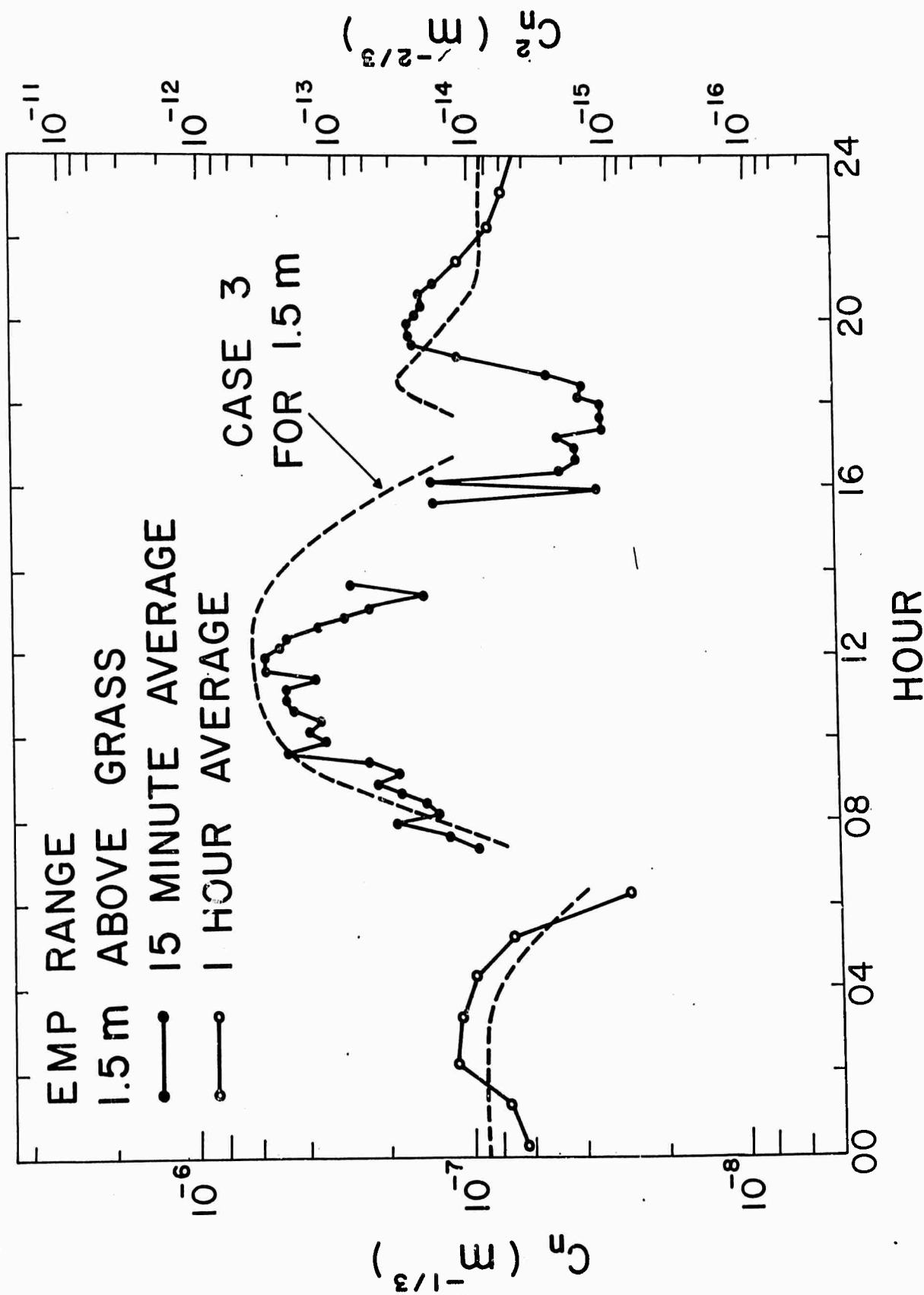


Figure 10 - Test of case 3 with measurements made at the U. S. Army Ballistic Research Laboratories, May 27 and 28, 1971.

Winter trends of C_n are shown in Figs. 3 and 4, for which all air and surface temperatures are assumed below freezing. The sensible heat fluxes and thus C_n 's would be different above a thawing surface. Since the values of H in Figs. 3 and 4 only partially come from direct flux measurements, the values of C_n are the least reliable of the six cases presented here. Nighttime H over snow was estimated using Neiderdorfer's [Geiger, 1961] nocturnal mean of about 17 W m^{-2} . Also, temperature lapse rates measured by Geiger [1961] above snow indicate that -H and thus C_n gradually decrease during a clear night. Since during the daytime only a slight decrease of temperature with height above snow was measured, small estimates of H were used, and they were chosen to be in phase with the expected solar radiation. The magnitudes of H at night in Fig. 4 are smaller than for Fig. 3 because of the lessened emitted radiative flux and increased soil heat flux for the grassy surface. For unstable conditions in Fig. 4, H is greater than in Fig. 3 because of the increased absorption of solar radiation.

As shown in Fig. 9, measurements were taken to test the curves in Fig. 4. The measurements were made above a level, brown grass surface on the Electromagnetic Propagation Range (EMP Range) at the U. S. Army Ballistic Research Laboratories, Aberdeen Proving Ground, Maryland. The curves in Fig. 4 are shown to be reliable in Fig. 9, despite the low values of C_n between 1700 and 2400 hours caused by extremely low winds, a common but sometimes unpredictable occurrence.

In Fig. 5, C_n trends are shown for a wet, grassy surface in late spring or late summer, or in midsummer with a haze. The values of H chosen are typical of Central Europe [Geiger, 1961] and were obtained from measurements taken near Hancock, Wisconsin, by Wesely *et al.* [1970]. In Fig. 10 measurements of C_n above grass at the EMP Range, Aberdeen Proving Ground, Maryland, show that the predictions are accurate. Clouds caused low C_n 's from 1600 to 1800 hours. Predictions of C_n for a grassy, partially dry surface are shown in Fig. 6, where the values for H were chosen from Wesely's measurements near Davis, California. The H and

thus C_n estimates are typical for the Great Plains of the United States [Wyngaard *et al.*, 1971; Lettau and Davidson, 1971] or the Russian Steppes [Kallistratova and Timanovskiy, 1971; Zilitinkevich and Chalikov, 1968] provided the soil is wet beneath the top few centimeters and the grass is actively growing. The maximum nighttime C_n 's for both Figs. 5 and 6 occur an hour or two after sunset because evaporation continues to cool the surface.

Figs. 7 and 8 are extremely dry climates in the winter and summer, respectively. However, the values of H and C_n above grassy plains or steppes during a summer drought could approach those in Fig. 7 as the soil dries out and the grass turns brown. The values of H in Fig. 7 are taken directly from measurements made in Pampa de La Joya, Peru, by Stearns [1969]. Daytime values of H in Fig. 8 were taken from Vehrencamp's [1953] measurements at El Mirage, California, but since his nighttime values of wind speed and H were low, the nighttime values of H and C_n in Fig. 8 were taken from Fig. 7. The predicted C_n 's of Fig. 8 have been partially substantiated by measurements made by T. H. Pries at the U. S. Army Atmospheric Sciences Laboratory at White Sands Missile Range where preliminary evaluation of data collected in early 1972 show peaks near $C_n = 7 \times 10^{-7} m^{-1/3}$ at a 3-meter height.

The trends drawn in Figs. 3 through 8 are poor climatological models because several assumptions of "ideal" conditions are made. Large reductions in C_n occur whenever clouds obscure the sun or a significant portion of the sky at night. Reductions in visibility also lower the radiation absorbed at the surface and thus the C_n . Real diurnal curves are rarely as smooth as these "ideal" ensemble averages since wiggles, usually caused by nonstationary winds and other synoptic effects, can be expected. Equations 9 and 10 are valid only when the site is flat and homogeneous upwind from the measurement site. Estimates of the necessary fetch have been determined by several authors [Elliot, 1958; Brooks, 1961; Panofsky and Townsend, 1964; Taylor, 1969] to be from 50 to 100 times the height of the sample. If intermittency is strong, which

is most likely to occur at heights greater than 4 meters, then equation 13 is invalid and C_n will be overestimated by equations 9 or 10. Finally discontinuities of C_n do not exist as shown on the graphs for the neutral conditions near sunrise and sunset. The curves should approach zero, but C_n is usually finite because the "fleeting moment" at which there are no temperature fluctuations is included in a ten-to-thirty-minute average essential for point measurements in the atmospheric surface layer. The curves for different heights should be slightly out of phase because of *Swinbank's* [1964] observation that the moment at which the temperature fluctuations go to zero at the surface may be as much as 15 minutes sooner than at 16 meters.

CONCLUSION

The diurnal cycle predictions of C_n presented in this paper indicate the magnitude of refractive index fluctuations in the inertial subrange of the atmospheric surface layer over land. These values of C_n can be used in the various theoretical expressions that give the magnitude of amplitude and phase alterations of electromagnetic radiation through a thermally turbulent atmosphere. Low intermittency is assumed, and thus the results are most applicable to heights less than 4 meters. For a given climate, season and surface type the values of C_n given here are the maximum expected since cloudless skies, excellent visibility and nearly optimum wind are assumed. Thus the diurnal cycles in Figs. 3 through 8 should be used only as rough approximations for clear skies, and during propagation experiments measurements of C_n should be made. The simple, direct, structure function approach of equation 1 is more desirable than the indirect methods using equations 9 and 10, which rely upon semiempirical relationships. Regardless of the measurement technique chosen, one measurement usually suffices to determine C_n at any height, since as shown by equation 9, C_n is proportional to $z^{-1/3}$ in the atmospheric surface layer.

Future work in determining the diurnal behavior of C_n in the atmospheric surface should include a study of the influence of water vapor fluctuations above oceans, lakes, and swamps. Recent flux measurements by *Pond et al.* [1971] above the sea show $\beta \sim 0.1$ within 10° of the equator, and according to equation 10 an estimate of C_n based upon a direct measurement of C_T would be too large by 30%. A smaller effect is expected at greater latitudes since seasonally averaged values of β increase to nearly 0.5 at 70°N [*Sellers*, 1965]. The value of β above oceans near shores and above small bodies of water can be exceptionally small and is usually negative during the daytime if the nearby land regions are dry [*Geiger*, 1961; *Sellers*, 1965]. Thus, at selected times and places water vapor fluctuations can greatly influence C_n .

REFERENCES

- Brooks, F. A., Need for measuring horizontal gradients in determining vertical eddy transfers of heat and moisture, *J. Meteorol.*, 18, 589, 1961.
- Businger, F. A., J. C. Wyngaard, Y. Izumi, and E. F. Bradley, Flux-profile relationships in the atmospheric surface layer, *J. Atmos. Sci.*, 28, 181, 1971.
- Chalfee, R. F., Anamalous dispersion calculated for atmospheric water vapor, *Appl. Opt.*, 7, 1652, 1968.
- Corrsin, S., On the spectrum of isotropic temperature fluctuations in an isotropic turbulence, *J. Appl. Phys.*, 22, 469, 1951.
- Elliot, W. P., The growth of the atmospheric internal boundary layer, *Trans. AGU*, 6, 1048, 1958.
- Fleagle, R. G., The optical measurement of lapse rate, *Bull. Amer. Meteorol. Soc.*, 31, 51, 1950.
- Geiger, R., *The Climate Near the Ground*, 611 pp., Harvard University Press, Cambridge, Mass., 1966.
- Haugen, D. A., J. C. Kaimal, and E. F. Bradley, An experimental study of Reynolds stress and heat flux in the atmospheric surface layer, *Quart. J. Roy. Meteorol. Soc.*, 168, 1971.
- Kallistratova, M. A., and D. F. Timanovskiy, The distribution of the structure constant of refractive index fluctuations in the atmospheric surface layer, *Izv. Acad. Sci. USSR Atmos. Oceanic Phys.*, Engl. Trans., 7, 46, 1971.
- Lawrence, R. S., G. R. Ochs, and S. F. Clifford, Measurements of atmospheric turbulence relevant to optical propagation, *J. Opt. Sci. Amer.*, 60, 826, 1970.

- Laykhtman, D. L., and S. M. Ponomareva, On the ratio of the turbulent transfer coefficients for heat and momentum in the surface layer of the atmosphere, *Izv. Acad. Sci. USSR Atmos. Oceanic Phys.*, Engl. Trans., 5, 719, 1969.
- Lettau, H.H., and B. Davidson (Ed.), *Exploring the Atmosphere's First Mile*, vol. 2. *Site Description and Data Tabulation*, 377-578, Pergamon Press, New York, 1957.
- List, R. J., *Smithsonian Meteorological Tables*, 527 pp., Smithsonian Institution, Washington, 1958.
- Livingston, P. M., P. H. Deitz, and E. C. Alcaraz, Light Propagation through a turbulent atmosphere: measurements of the optical-filter function, *J. Opt. Soc. Amer.*, 60, 925, 1970.
- Lumley, J. L., and H. A. Panofsky, *The Structure of Atmospheric Turbulence*, 239 pp., John Wiley, New York, 1964.
- McBean, G. A., R. W. Stewart and M. Miyake, The turbulent energy budget near the surface, *J. Geophys. Res.*, 76, 6540, 1971.
- Obukhov, A. M., Structure of the temperature field in turbulent streams, *Izv. Akad. Nauk. SSSR Ser. Geofiz.*, 13, 58, 1949.
- Panofsky, H. A., The spectrum of temperature, *Radio Sci.*, 4, 1143, 1969.
- Panofsky, H. A., and A. A. Townsend, Change of terrain roughness and the wind profile, *Quart. J. Roy. Meteorol. Soc.*, 90, 240, 1964.
- Pond, S., G. T. Phelps, J. E. Paquin, G. Mcbean, and R. W. Stewart, Measurements of the turbulent fluxes of momentum, moisture and heat over the ocean, *J. Atmos. Sci.*, 28, 901, 1971.
- Record, R. A., and H. E. Cramer, Turbulent energy dissipation rates and exchange processes above a non-homogeneous surface, *Quart. J. Roy. Meteorol. Soc.*, 92, 519, 1966.
- Sellers, W. D., *Physical Climatology*, 272 pp., University of Chicago Press, Chicago, 1965.

- Stearns, C. R., Surface heat budget of the Pampa de La Joya, Peru, *Mon. Weather Rev.*, 97, 860, 1969.
- Stearns, C. R., The effect of time-variable fluxes on mean wind and temperature profile structure, *Boundary Layer Meteorol.*, 1, 289, 1971.
- Swinbank, W. C., The exponential wind profile, *Quart. J. Roy. Meteorol. Soc.*, 95, 77, 1969.
- Tatarski, V. I., *Wave Propagation in a Turbulent Medium*, 285 pp., Dover, New York.
- Taylor, P. A., On wind and shear stress profiles above a change in surface roughness, *Quart. J. Roy. Meteorol. Soc.*, 95, 77, 1969.
- Tsvang, L. R., Measurements of temperature pulse frequency spectra in the surface layer of the atmosphere, *Izv. Acad. Nauk. SSSR Ser. Geofiz.*, Engl. Transl., 8, 833, 1960.
- Vehrencamp, J. E., Experimental investigation of heat transfer at an air-earth interface, *Trans. AGU*, 34, 22, 1953.
- Wesely, M. L., G. W. Thurtell, and C. B. Tanner, Eddy correlation measurements of sensible heat flux near the earth's surface, *J. Appl. Meteorol.*, 9, 45, 1970.
- Wyngaard, J. C., and O. R. Coté, The budgets of turbulent kinetic energy and temperature variance in the atmospheric surface layer, *J. Atmos. Sci.*, 28, 190, 1971.
- Wyngaard, J. C., O. R. Coté, and Y. Izumi, Local free convection, similarity, and the budget of shear stress and heat flux, *J. Atmos. Sci.*, 28, 1171, 1971.
- Wyngaard, J. C., Y. Izumi, and S. A. Collins, Behavior of the refractive-index-structure parameter near the ground, *J. Opt. Soc. Amer.*, 61, 1646, 1971.

Zilitinkevich, S. S., and D. V. Chalikov, The use of profile observations to calculate vertical turbulent fluxes in the atmospheric boundary layer, *Izv. Acad. Sci. USSR Atmos. Oceanic Phys.*, Engl. Trans., 4, 438, 1968.

Zubkovskiy, S. L., and B. M. Koprov, On the turbulent energy balance in the boundary layer of the atmosphere, *Izv. Acad. Sci. USSR Atmos. Oceanic Phys.*, Engl. Trans., 6, 589, 1970.